OVERVIEW OF THE NSNS TARGET STATION*

Tony A. Gabriel, John N. Barnes, Lowell A. Charlton, James DiStefano, Ken Farrell, John Haines,
Jeffrey O. Johnson, Louis K. Mansur,
Steve J. Pawel, Moshe Siman-Tov, Rusi Taleyarkhan, Mark W. Wendel
Oak Ridge National Laboratory , P. O. Box 2008, Oak Ridge, Tennessee 37831, USA
Ray S. Booth, Thomas J. McManamy, Mark J. Rennich, Warren Sharp
Engineering, Lockheed Martin Energy Systems, Inc., P. O. Box 2009, Oak Ridge, Tennessee 37830, USA

To be presented at the
American Nuclear Society
1997 Annual Meeting
Orlando, Florida
June 1-5, 1997

Managed by Lockheed Martin Energy Research Corp. for the U.S. Department of Energy under contract no. DE-AC05-960R22464.

OVERVIEW OF THE NSNS TARGET STATION

Tony A. Gabriel, John M. Barnes, Lowell A. Charlton, James Distefano, Ken Farrell, John Haines, Jeffrey O. Johnson, Louis K. Mansur, Steve J. Pawel, Moshe Siman-Tov, Rusi Taleyarkhan, Mark W. Wendel
Oak Ridge National Laboratory, P. O. Box 2008, Oak Ridge, Tennessee 37831, USA

Ray S. Booth, Thomas J. Mcmanamy, Mark J. Rennich, Warren Sharp
Engineering, Lockheed Martin Energy Systems, Inc., P. O. Box 2009, Oak Ridge, Tennessee 37830, USA

ABSTRACT

The technologies that are being utilized to design and build a state-of-the-art neutron spallation source, the National Spallation Neutron Source (NSNS), are discussed. Emphasis is given to the technology issues that present the greatest scientific challenges. The present facility configuration, ongoing analysis and the planned hardware research and development program are also described.

I. INTRODUCTION

In many areas of physics, materials and nuclear engineering, it is extremely valuable to have a very intense source of neutrons so that the structure and function of materials can be studied. One facility proposed for this purpose is the National Spallation Neutron Source (NSNS). This facility will consist of two parts: 1) A high-energy (~1 GeV) and high powered (~1 MW) proton accelerator, and 2) A target station which converts the protons to low-energy ($\lesssim$ 2 eV) neutrons and delivers them to the neutron scattering instruments.

This paper deals with the second part, i.e., the design and development of the NSNS target station and the scientifically challenging issues. Many scientific and technical disciplines are required to produce a successful target station. These include engineering, remote handling, neutronics, materials, thermal hydraulics, and instrumentation. Some of these areas will be discussed below.

II. TARGET STATION CONFIGURATION AND MAINTENANCE

The target and experimental systems for the NSNS are located in a single building. As shown in Fig. 1, the target is positioned within an iron and concrete shielding monolith approximately 12 m in diameter. The proton beam enters horizontally and moderated neutrons used by the scattering instruments exit through 18 neutron beam tubes projecting from the sides. The majority of the 50 m x 75 m building is reserved for the scattering instruments located on the neutron beam lines, however, remote handling hot cells projecting from the back of the shielding are provided for handling the activated target, moderator and reflector components. This region also contains utilities used for the target. Another cell for utility systems is located beneath the main floor level.

The target facility can be segregated into four areas for discussion:

- target assembly including the moderators and reflectors,
- neutron beam tube systems
- remote handling systems
- target system controls

A. Target

1. Liquid Target Material. The reference design for the NSNS incorporates mercury as its target material. Previous efforts by the European Spallation Source (ESS) team have been used extensively in developing the NSNS mercury target station [Ref. 1]. A heavy liquid metal target was selected over a water cooled solid target because (1) increased power handling capability is possible with a liquid target, (2) the liquid target material lasts the entire lifetime of the facility, and (3) the radiation damage lifetime of a liquid target system, including its solid material container, should be considerably longer. The first advantage is due to the large power loads that can be convected away from the beam-target interaction region with a flowing liquid target. The second advantage results from avoiding the radiation damage that would occur in a solid target material, which eventually

Fig. 1: Cutaway view of target facility

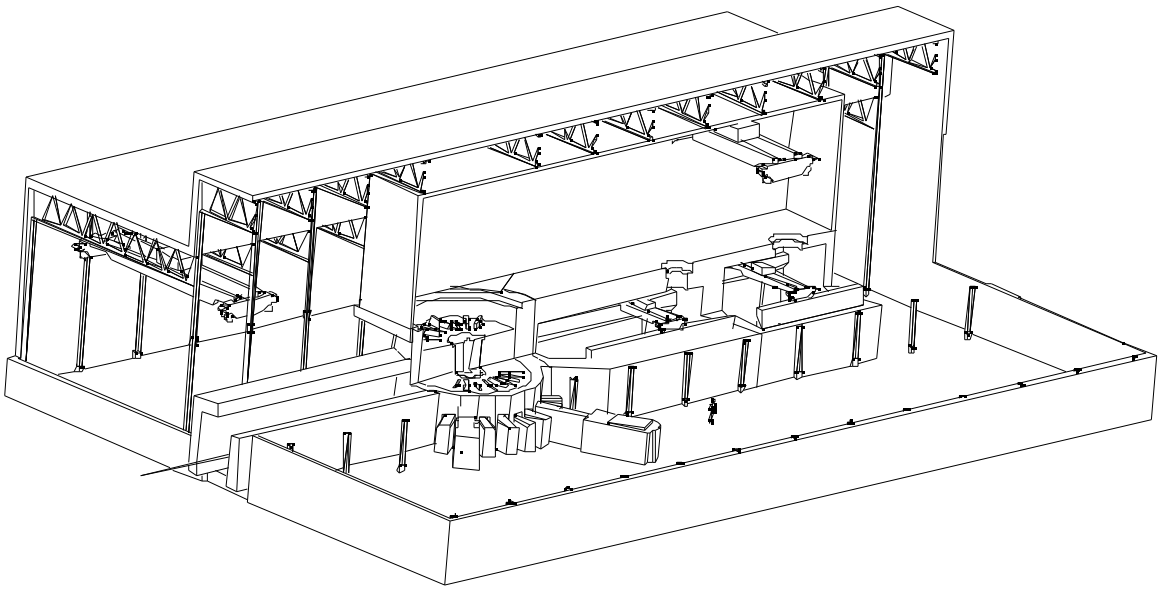

leads to embrittlement and fracture of the material. Liquid target vessels will still need to be replaced periodically due to radiation damage to its container structure, but the liquid target material can be reused. The third advantage - longer irradiation lifetime - results from two effects. The target structural material used to enclose the liquid targetcan be selected based on its structural properties and resistance to radiation damage, independent of its neutron production capability. This is similar to the situation for a solid target. However, with a liquid target, there is no solid material in the highest neutron flux regions. Further, the peak displacement damage rate in the window of a liquid target is greatly reduced compared to the peak value in a solid target because the high energy displacement cross-section of tungsten is substantially larger than that of stainless steel, for example.

Mercury was also selected as the reference liquid target material because it: (1) is a liquid at room temperature, (2) has good heat transport properties, and (3) has high atomic number and mass density resulting in high neutron yield and source brightness. One significant result from recent neutronic analysis studies has been that the neutron flux from a short-pulse (~1 μs) neutron source is substantially greater for a mercury target than for either water-cooled tungsten or tantalum targets especially at power levels greater than 1 MW (see section 3).

2. Mercury Target Design Concept. The mercury target design configuration, shown in Fig. 2, has a width of 400 mm, a height of 100 mm, and a length of 650 mm. The mercury is contained within a structure made from 316-type stainless steel. Mercury enters from the back side (side outermost from the proton beam window) of the target, flows along the two side walls to the front surface (proton beam window), and returns through a 224 mm x 80 mm rectangular passage in the middle of the target. Also being considered is the opposite flow, i.e. in through the 224 mm x 80 mm passage and out the two side walls. The target window, i.e., portion of the target structure in the direct path of the proton beam is cooled by mercury which flows through the passage formed between two walls of a duplex structure. In this way, the window cooling and transport of heat deposited in the bulk mercury are achieved with separate flow streams. This approach is judged to be more reliable and efficient (minimal pressure drop and pumping power) than using the bulk mercury to cool the window. Also, the duplex structure used for the window has significant structural advantages that help to sustain other loads. Beside serving as flow guides, the baffle plates used to separate the inlet and outlet flow streams are also important for maintaining the structural stability of the target.

A shroud (safety container) is provided around the mercury target to guide the mercury to a dump tank in the event of a failure of the target container structure. The shroud is a water-cooled duplex structure made from austenitic, 316-type, stainless steel.

B. Target Station

1. Configuration. The overall configuration for the liquid target system is shown in Fig. 3. The mercury target and the water cooled shroud, which are subject to

intense interactions with the proton beam, must be replaced on a regular basis. For this reason, all major liquid target system components, except the dump tank, are located on a mobile cart, which is retracted into the target hot cell for maintenance activities. The mercury contained in the target system is drained to the dump tank prior to retracting the target assembly.

intermediate loop. In addition to this primary heat exchanger, the mercury flow loop also includes piping, valves, fittings, pumps, expansion tanks, and mercury processing equipment. The secondary (water) loop transports the heat to a secondary heat exchanger located in the floor below the target hot cell. The tertiary flow stream utilizes process water.

Fig. 2: NSNS Mercury Target

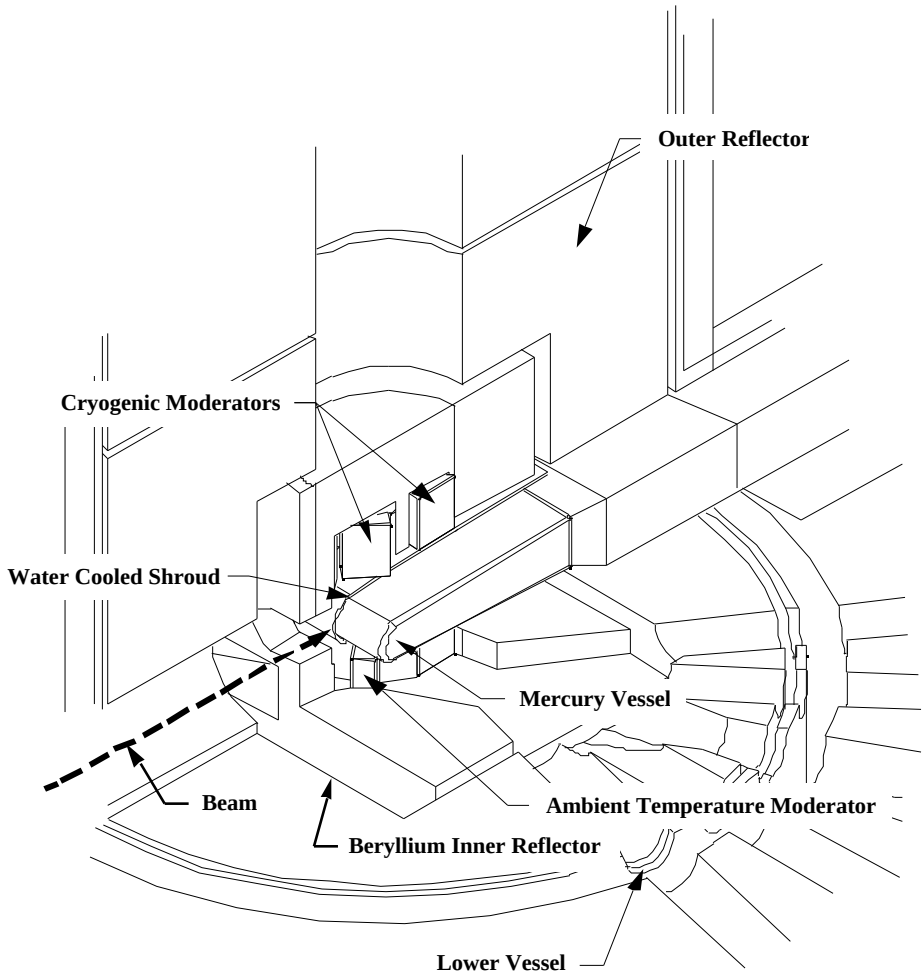

The heat deposited in the mercury target is transported away in the flowing mercury loop to a primary heat exchanger that is located on the target cart assembly, outside the target region shielding. The primary heat exchanger is a shell and tube type with mercury flowing in the tube side and the secondary coolant, i.e., demineralized water, flowing in the shell side. The tubes in this heat exchanger are a special, double-walled type which reduces the probability of a mercury leak into the

The water-cooled shroud is provided around the mercury target to guide the mercury to a dump tank in the event of a failure of the target vessel. This shroud is formed from a duplex structure similar to the mercury target vessel and is also made from stainless steel.

A 65 ton target shield plug, shown in Fig. 3, is designed to shield the equipment located in the target hot cell from the high energy, forward scattered neutrons

produced in the mercury target. The shield plug, which is removed as part of the target assembly during maintenance operations, is constructed from water-cooled, bulk iron encased in a stainless steel liner.

The cart assembly supports all of the mercury flow loop equipment, and provides the means for transporting the target assembly into the target hot cell.

The mercury dump tank is located below all other components in the mercury system thus ensuring that most of the mercury can be drained to the dump tank even in a passive (failure of the electric power system) situation. A gas purge system is also utilized under normal circumstances to provide more complete removal of the mercury from the target systems to the dump tank. The capacity of the dump tank is 1 m^3, which is slightly larger than the mercury inventory in the remainder of the system. The tank is actively cooled with a gas stream to remove the nuclear afterheat in the mercury.

2. Ambient Temperature Moderators. Fig. 2 shows the two light water moderators planned for the NSNS. They are located in wing geometry below the mercury target and water-cooled shroud. The moderator vessel is made from aluminum alloy-6061. The upstream moderator has a thickness of 50 mm, relative to the proton beam, and is decoupled and poisoned to give high temporal resolution of the neutron flux. The second moderator is 100 mm thick and is coupled to produce higher neutron intensity but with less temporal resolution. Both moderators are approximately 120 mm wide and 150 mm high.

The overall heat load in the ambient moderators is estimated to be 4 kW (2 kW per moderator) based on extrapolations from ISIS and ESS data. This heat load results in an overall temperature rise of less than 1 °C for a nominal flow rate of 2 L/s.

3. Cryogenic Moderators. In addition to the two ambient temperature moderators located beneath the target, two cryogenic moderators, cooled with supercritical hydrogen, are located above the target as shown in Fig. 2. This configuration improves the cooling and warming characteristics of the moderators. Mechanically circulated supercritical hydrogen gas at a pressure of 1.5 MPa was chosen for the moderators because it improves the cooling operation, eliminates boiling and adds flexibility in operation. The hydrogen is maintained at supercritical pressures in all parts of the loop during normal operation.

4. Reflector Systems. As identified in Fig. 2, the reflector system consists of two major subsystems, namely the inner reflector and the outer reflector. The inner reflector consists of a stainless steel case packed with beryllium rods and cooled with heavy water. Neutron decouplers made from boral are mounted on the inner surface of the case. The heavy water flow loop includes appropriate equipment, such as piping, valves, an expansion tank, connectors, pumps, ion exchangers, and instrumentation. The system is designed with connectors to allow disconnection and removal of the reflector assembly vertically into a shielded cask for transport to the target assembly hot cell.

The outer reflector consists of iron or nickel shielding which surrounds the beryllium reflector assembly and is contained within a 2 m diameter safety vessel.

5. Neutron Beam Transport Systems. The neutron beam tube systems provide the paths for moderated neutrons to travel through the bulk shielding to the scattering instruments. The configuration assumed at present consists of 18 beam lines looking at the four moderators as shown in Figures 1 and 2. Each moderator face which is viewed illuminates three beam lines, one normal to the face and two at plus or minus 13.75 degrees. The upper and lower forward moderators have two faces viewed and the two rear moderators each have one face viewed for a total of 6 viewed faces. This arrangement allows a 70 degree arc for the proton beam entrance region and a similar 70 degrees arc for the remote maintenance systems at the rear of the target.

A neutron beam shutter concept similar to the ISIS vertical shutter design is planned. The shutters are in the form of stepped rectangular slabs. In the open position a hole in the shutter aligns with the neutron beam flight path and cross section. The shutter is lowered approximately 500 mm to close. This puts approximately 2 m of shielding in the neutron flight path. The drive for the shutters will be from the top. Each shutter will be made from several sections to reduce the height above the top of the bulk shielding required for removal and the size of the shielded flask required for transport. All shutters will be the same, except for the difference in beam elevation required between beam lines viewing the upper or lower moderators. The weight of one shutter assembly is approximately 25 tons.

The neutron beam lines require shielding outside of the bulk target shield. This shield is both for personnel protection and also to reduce the background noise in instruments. It is assumed that standard modules will be developed to allow sections to be added or removed, depending on the requirements and locations of the scattering instruments.

6. Remote Handling Systems. Optimization of both the operating availability and predictability, while protecting personnel, is the primary goal of the maintenance systems for NSNS. Several techniques proven in successful facilities throughout the world are applied to assist the operators in meeting the operating goals. These include designing equipment from the

earliest stages to reduce the need for remote handling. Operating equipment are packaged in modular assemblies designed to be replaced with on-site spares. This enables operations to continue while time-consuming repairs are performed in off-line facilities.

The As Low As Reasonably Achievable (ALARA) principle is used as guidance for all personnel and contamination control operations in NSNS. Thus, activated and contaminated equipment are shielded for transport around the facility and to the permanent storage site. Areas of potential contamination are isolated by seals and valves. Repair and replacement of active remote, however; personnel may enter the cell following extensive cleanup. The cell measures 6 meters wide, 15.5 meters long and 6.2 meters high.

The enclosed, unshielded high-bay above the target system and maintenance cells will provide the primary means of handling components in the target system. It measures 8 meters wide, 20 meters high and extends 55 meters. A 50 ton bridge crane provides access to all of the maintenance cells, storage wells and the transportation bay. The access bay is normally accessible to personnel, consequently all activated components will be shielded and contained during operations and during component

Fig. 3: Target System Configuration

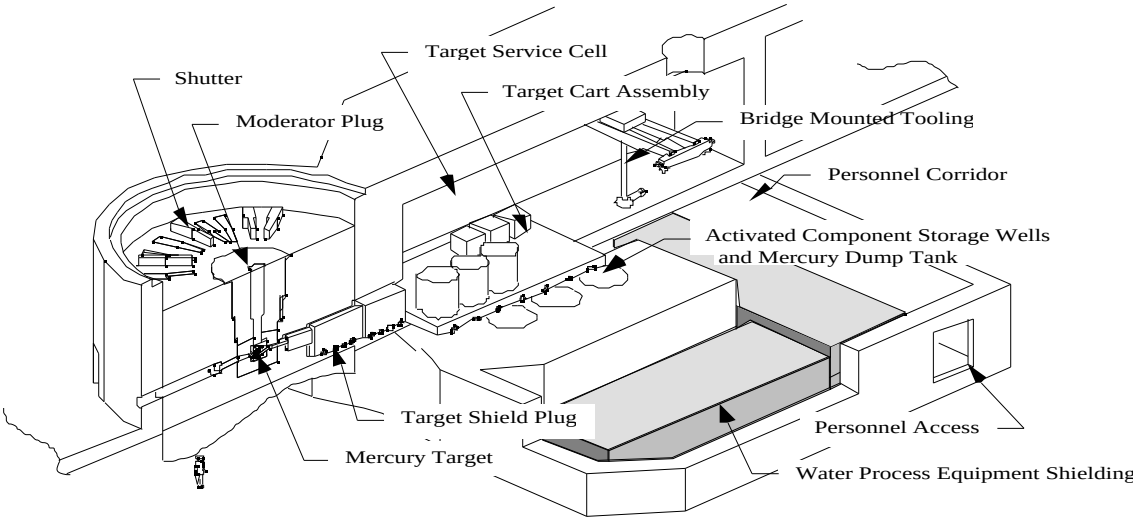

components are accomplished in the hot cell adjoining the target shielding stack as identified in Fig. 3.

A target service cell is located behind the target assembly for the purpose of maintaining the highly activated target components. It measures 6 meters wide by 15.5 meters long by 5.2 meters high. All work is performed via remote handling techniques behind concrete shielding walls. Conventional remote handling tools such as telerobotic manipulators, CCTV and special lighting are used to assist with the replacement of target components. Modular packaging of the components is used to reduce down-time.

A general maintenance cell is located behind the target service cell primarily to maintain the moderator/reflector plug, proton beam window, neutron guide tubes and shutters. Generally all operations will be transfers between the hot cells. In addition, utility and instrument connections to the vertical access plugs (i.e. shielding, moderators, reflectors and proton beam window) are routed in shielded trenches in the floor of the bay.

III. NEUTRONICS

The neutronic behavior of the target system can be obtained by using Monte Carlo techniques to track the progress of various subatomic particles as they proceed through the target. For the work presented here the codes HETC95 [Ref. 2] and MCNP [Ref. 3] were used. The codes were coupled in order to provide the proper source for the low energy MCNP calculations. Various parameters were calculated to measure the neutronic performance of the target design. The two parameters which were most often tracked in the study reported below

were the neutron current (J) passing into the neutron beam channels which lead to the experimental area and the time width (W) of the beam channel neutron pulse.

For this first study, a proton energy of 1.7 GeV, a power of 1 MW, a repetition rate of 60 Hz and a proton pulse width of .5 μsec was assumed. The target assembly is shown in Fig. 4. The beryllium reflector surrounds the neutron producing mercury target, the moderators, which slow the produced neutrons to useful energies (the top cryogenic moderators are filled with liquid hydrogen and the bottom ambient moderators with water), and the neutron beam channels which guide the neutrons to the experimental area. In Fig. 4, the beryllium has dimensions 0.9 m x 0.9 m x 1.008 m with the square plane perpendicular to the proton beam direction. The largest dimension of the proton beam channel is 120 mm by 320 mm. The Hg target has a rectangular cross section width of 300 mm and a height varying from 100 mm upstream to 150 mm at the extreme downstream end. The length is 640 mm.Various moderator parameters are show in Table 1.

Fig. 4: Target assembly enclosed in the Beryllium reflector.

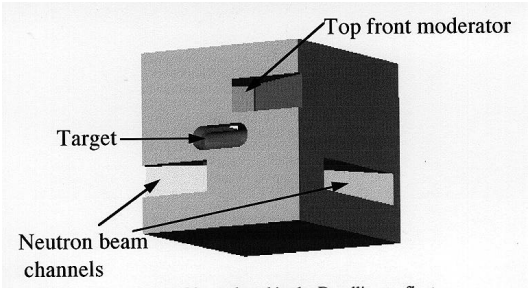

A. Mercury Target

The neutronic superiority of Hg over two other commonly considered targets is shown in Table 2. This increase in neutronic performance will be slight at 1 MW but substantial at 5 MW due to the increase in the H_2O cooling needed for the solid target at 5 MW. The hydrogen in the water thermalizes some of the neutrons within the W or Ta target area. Since both W and Ta have large capture cross sections these thermalized neutrons are captured and therefore lost. Calculations of the neutron flux for a 5 MW target station are shown in order to facilitate a comparison with a different study done for ESS. The results of this study are also shown. As may be seen, Hg gives a larger neutron flux than either Ta or W. This is true for both cryogenic (liquid H_2) and ambient (H_2O) moderators. Comparison of the neutron spectrum and pulse showed virtually identical characteristics except for the additional neutrons given by the Hg target.

Table 1: Moderator Parameters (unless stated otherwise in text)

Moderator	Dimensions (mm)	Decoupler Thickness (mm)	Poison Thickness (mm)
Top Upstream (Faces 1&2)	120 x 150 x 50	1. Cd	0.05 Gd
Top Downstream (Faces 3&4)	120 x 150 x 50	1. Cd	0.05 Gd
Bottom Upstream (Face 5)	120 x 150 x 50	1. Cd	0.05 Gd
Bottom Downstream (Face 6)	120 x 150 x 100	1. Cd	0.05 Gd

The size of the moderator face from which the neutrons enter the beam channel is given by the first two dimensions in the second column.

B. Moderator Enhancement

It is desirable to maximize the neutron current (J) emerging from the moderator and to minimize the time width (W) of the neutron pulse. The results discussed in this section concern the use of moderator poisoning and

Table 2. Comparison of neutron fluxes at the moderator faces for Hg, W and Ta Targets at 5 MW

Cryogenic				
	NSNS		ESS	
Target	φ_{th}	R	φ_{th}	R
Hg	2.94×10^{14}	1.35	3.91×10^{14}	1.23
W	2.54×10^{14}	1.17	3.53×10^{14}	1.10
Ta	2.17×10^{14}	1.00	3.19×10^{14}	1.00

Ambient				
	NSNS		ESS	
Target	φth	R	φth	R
Hg	3.35×10^{14}	1.35	2.29×10^{14}	1.51
W	2.91×10^{14}	1.17	1.67×10^{14}	1.10
Ta	2.48×10^{14}	1.00	1.52×10^{14}	1.00

Units: φ_{th}(n/cm^2-sec)

ESS results from D. Filges, R. D. Neef, and H. Schaal "Nucl. Studies of Different Target Systems for ESS," ICANS-XIII.

NSNS "effective" fluxes were converted from 2π steradian current calculations. The differing distances from the target to the moderator were also corrected for.

R is the ratio of the flux from the given target to that from a tantalum target.

The neutron current has been integrated from 0 to .414 eV for Ta and W. 35% D_2O cooling has been assumed for the NSNS calculations and 25% for the ESS calculations. This is considered realistic.

moderator decoupling to reduce the time width of the neutron pulse. These methods successfully reduce the width but they also reduce the neutron current. Thus a trade off is required between the neutron current and the width of the pulse. The best trade off is determined by the target output requirements.

In order to better understand the width reduction produced by each method, the energy distribution produced will be shown first. In Fig. 5, the number of neutrons per incident proton leaving a moderator face is shown versus the energy in meV. The face used is one of the two on the front top cryogenic moderator (the two faces yield virtually identical results). Both poisoning and decoupling reduce the neutron current and using both reduces it further than using either separately. Poisoning (accomplished by gadolinium with a cut-off energy of .1-.2 eV) changes the neutron spectrum only for energies

Fig. 5: Neutron energy distribution from the face of the cryogenic moderator. C = coupled, P = poisoned, D = decoupled, P-D = poisoned and decoupled.

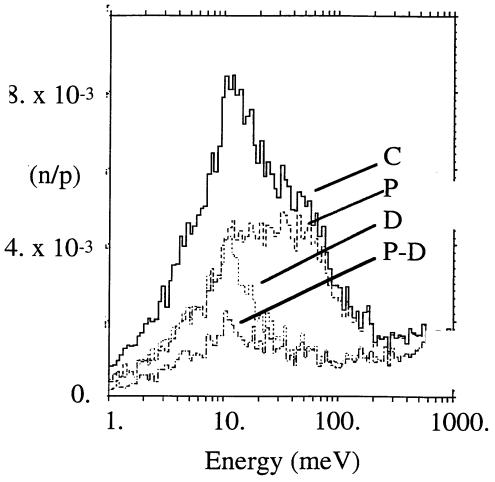

Fig. 6: Thermal neutron pulse from the face of the front front cryogenic moderator.

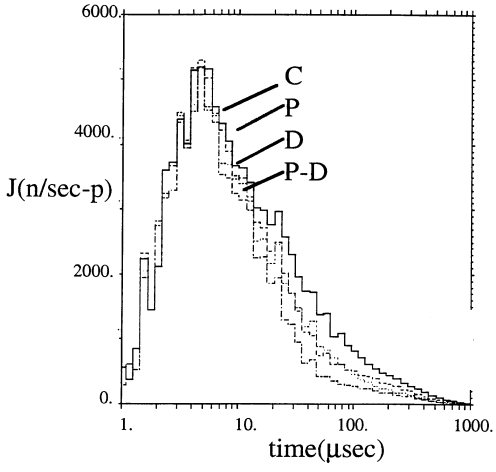

$\lesssim$ .1-.2 eV. Neutron capture in Gd above this energy is small. It may also be seen that decoupling modifies the neutron spectrum only for energies below the cadmium cutoff energy of ~.4-.6 eV (decoupling includes the use of a Cd neutron beam tube liner).

These same effects can be seen for the ambient moderators except they are much less pronounced. This is because the peak in the energy distribution is located at a much higher energy relative to the cut off energies of both cadmium and gadolinium which means that a much smaller proportion of the neutrons that eventually moderate to the peak energy are affected by the poisoning and the decoupling. This produces a smaller effect. The threshold for decoupling occurs at the cut-off energy for cadmium and the threshold for poisoning occurs at the cut off energy for gadolinium. These thresholds are, however, much farther above the peak in the coupled energy distribution for the cryogenic moderator than for the ambient moderator.

The change in the shape of the neutron pulse for the cryogenic moderator due to poisoning and decoupling can be seen in Fig. 6. The decoupling and poisoning preferentially affect the low energy particles which take longer to reach the moderator face. At small times all pulses are approximately the same. Only at large times do the poisoning and decoupling reduce the current and thus produce a smaller time pulse width as desired. The changes produced when an ambient moderator is considered are again smaller than for the cryogenic case. This is due to the same reasons discussed above. Time pulse distributions have also been calculated for various energy ranges, for example, 10 to 20 meV.

The total currents from the moderator faces together with the pulse widths are shown in Table 3.

IV. TARGET RESEARCH

A. Mercury Target Performance Evaluations

The mercury target and its enclosing structure must be designed to sustain the time-averaged power loads as well as the nearly instantaneous power deposition during single pulses. These time-averaged and single pulse loads are defined in Table 4. Since about 60% of the proton beam power is deposited in the target, the thermal-hydraulic system for the target is designed to remove a time-averaged power of 0.6 - 1.2 MW corresponding to proton beam powers of 1 - 2 MW. Since the pulse frequency is 60 Hz, the amount of energy deposited in the target during a single pulse is 10 - 20 kJ.

B. Handling of the Time-Averaged Power

Thermal-hydraulic performance parameters discussed in the following paragraphs are given for the 1 MW

Table 3: Maximum (J_{mx}) and Average (J_{av}) Currents and Pulse Widths (W) for the Front Cryogenic (Faces 1 and 2) and the Front Ambient (Faces 3 and 4) Moderators (Note that 2π current is given instead of 4π flux which can make the values appear ~4 smaller)

Neutron Currents and Pulse Widths						
	Coupled			Decoupled and Poisoned		
Face	J_{av} (n/cm^2-sec)	J_{mx} (n/cm^2-sec)	W (μsec)	J_{av} (n/cm^2-sec)	J_{mx} (n/cm^2-sec)	W (μsec)
1	6.73×10^{12}	9.53×10^{14}	38	1.90×10^{12}	8.17×10^{14}	15
2	6.66×10^{12}	9.20×10^{14}	38	1.73×10^{12}	7.83×10^{14}	14
3	7.06×10^{12}	1.74×10^{15}	30	3.28×10^{12}	1.60×10^{15}	17
4	7.87×10^{12}	1.91×10^{15}	26	3.97×10^{12}	1.80×10^{15}	17

The neutron current has been integrated from 0 to .414 eV.

Table 4. Power loads on the NSNS mercury target

Parameter	Value
Energy of protons (GeV)	1
Pulse duration (μs)	0.5
Pulse frequency (Hz)	60
Percent of beam power deposited in mercury target (%)	60
Time-Averaged Loads	
Beam current (mA)	1 - 2
Total proton Beam Power (MW)	1 - 2
Peak current density on target (A/m^2)	0.14 - 0.28
Peak beam power flux on target (MW/m^2)	140-280
Peak volumetric heating rate in mercury (MW/m^3)	400 - 800
Peak volumetric heating rate in window (MW/m^3)	50 - 100
Loads During a Single Pulse	
Energy per pulse (kJ)	10 - 20
Peak energy density in mercury (MJ/m^3)	6.7 - 13
Peak energy density in window (MJ/m^3)	0.83 - 1.7

proton beam case which is considered the baseline design value. Values for a 5 MW proton beam case, which is considered to be the power for a possible upgrade facility, are shown in parentheses. The time-averaged power must be transported from the target without excessive temperatures or stresses. This is achieved by flowing the mercury at a rate of 140 kg/s (710 kg/s). The resulting bulk (volume averaged) temperature rise in the mercury is 30°C (30°C). The general purpose computational fluid dynamics (CFD) code CFDS-FLOW3D [Ref. 4] was used to simulate the heat transfer and fluid dynamic processes in several preliminary design concepts for the mercury target.

Thermal-hydraulic analysis results for an initial simple test design concept that had a central baffle running horizontally through the midpoint of the target are shown in Fig. 7 for a 1 MW beam case. The target wall was assumed to be cooled with Hg flowing in a separate passage running in the space between the two plates in a duplex structure. Peak time-averaged velocity in the target is roughly 1.6 m/s (8.5 m/s).

As shown in Fig. 7, there is a time-averaged "recirculation zone" along the upper portion of the baffle in the region closest to the proton beam - very close to the peak heating region in the mercury target. It should be noted that this recirculation zone is in reality not a region of zero flow speed, but rather a region of flow where the velocity fluctuates about a zero average value. Despite this unfavorable situation, the peak temperatures shown in Fig. 7 for the mercury and stainless steel baffle in this "hot spot" region are quite manageable - - 161°C for the mercury and 173°C for the stainless steel. Even for a 5 MW beam, the corresponding temperatures of 163°C and 244°C, respectively, are probably tolerable.

Evaluations of the latest design concept discussed in the previous section are not available at this time. However, it is expected that temperatures will be somewhat lower in the latest design, because of the elimination of the central baffle and its consequent recirculation region.

C. Evaluation of the Thermal-Shock Loads

The interaction of the energetic proton beam with the mercury target leads to very high heating rates in the target. Although the resulting temperature rise is relatively small (a few °C), the rate of temperature rise is enormous (~10^7°C/s) during the very brief beam pulse (~ 1 μs). The resulting compression of the mercury will lead to the production of large amplitude pressure waves in the mercury that interacts with the walls of the mercury container, and the bulk flow field. Concerns exist in two main areas, (1) impact of the effects of the combination of thermal shock on the wall due to its direct heating from the proton beam and the loads transferred from the mercury compression waves, and, (2) impact of the compression-cum-rarefaction wave-induced effects such as fluid surging and potential cavitation. This has led to the conclusion that tests and analyses are required before using a liquid target (mercury) in the intense thermal load

Fig. 7: Flow and temperature distributions in a preliminary mercury target design concept for a 1 MW proton beam (enlargement at front of target shown).

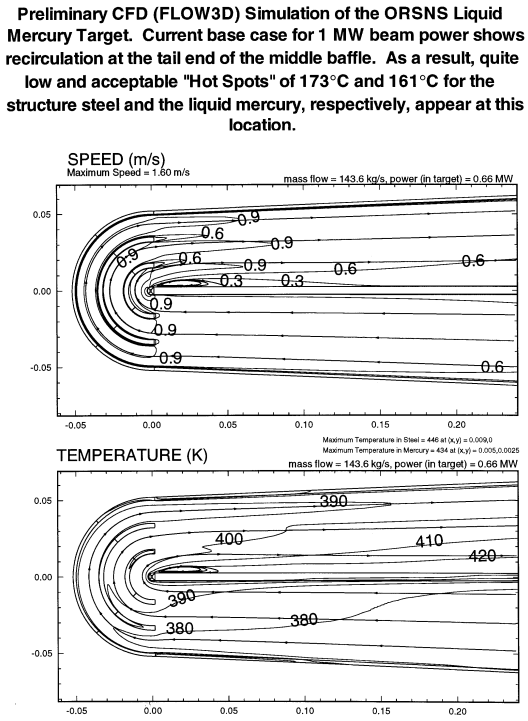

environment expected for a pulsed spallation neutron source.

The capability to understand and predict the propagation of the pressure pulses in the target (either liquid or solid) is considered to be critical for designing and constructing such a device. The CTH code [Ref. 5] system developed at Sandia National Laboratory is being used to model this situation. CTH is a three-dimensional, shock-physics code, sometimes loosely referred to as a hydrocode.

Current results indicate that the peak tensile stress in the stainless steel structure is found to be about 200 Mpa. This is roughly equal to the yield strength of solution annealed 316-type stainless steel. These results indicate that for a 5MW proton beam, the thermal shock stresses are a serious concern; however, at the reference NSNS beam power of 1MW, these stresses, although significant, are expected to be tolerable.

IV. MATERIALS TECHNOLOGY ISSUES FOR THE NATIONAL SPALLATION NEUTRON SOURCE TARGET STATION

High power spallation neutron sources like the NSNS will place significant demands on materials performance. The target system will be subjected to an aggressive environment that will degrade the properties of materials. Indeed, the satisfactory performance of materials for sufficiently long time periods will determine the viability of the target station for the facility. Components at the heart of the facility include the liquid target container and return hull, beam windows, support structures, moderator containers and beam tubes, for example. A recent workshop summarized the present state of knowledge of materials for spallation sources, and began implementing materials R&D programs for the NSNS and ESS facilities [Ref. 6]. The materials R&D program for the NSNS is oriented toward materials qualification. By this is meant informed selection of materials based on existing experimental data and analysis, testing in actual and partially simulated application environments, lifetime estimates for the NSNS environment, and iteration and optimization of properties to improve performance. The program is structured around technical areas expected to be key to the design, fabrication, and performance of the target station. The five overlapping areas can be termed *radiation effects, compatibility, materials engineering, in-service surveillance and technical support.*

Most of the present section will concentrate on radiation effects and compatibility. Materials engineering refers to the work necessary to translate knowledge gained

in these areas into fabrication of components so that the necessary properties are achieved. Questions include, for example, methods of welding and joining, assembly, heat treatments, and quality assurance. An in-service surveillance program is being developed to monitor and improve the performance of actual components. More importantly, standard specimens in a well-characterized environment that are more suitable than service components for testing and characterization will be irradiated. Parameters to be monitored include dose, dose rate, temperature, and target chemistry. The technical support function covers both the R&D phase of the project as well as the detailed design and construction phases. It gives a wide variety of support to the project that includes supplying materials properties data to target station engineers, and the solution of numerous applications-specific issues expected to arise. Test on radiation effects are currently underway at LANSCE.

VI. CONCLUSIONS

Preliminary design and analysis indicate that a very attractive short-pulse neutron source operating at 1 MW of proton beam power can be constructed for the NSNS using liquid mercury as the target material. Research and development activities have been identified to validate design concepts and to allow future upgrades to higher power levels. Reasonable design configurations have been proposed for major component assemblies and remote handling concepts developed.

REFERENCES

1. G. S. Bauer, "ESS-Liquid Metal Target Studies," ESS95-33T (October 1995).

2. T. A. Gabriel et al., "CALOR87: HETC87, MICAP, EGS4, and SPECT, A Code System for Analyzing Detectors for Use in High Energy Physics Experiments," *Proceedings of the Workshop on Detector Simulation for the SSC*, Argonne National Laboratory, August 24-28, 1987.

3. J. F. Briesmeister, Ed. "MCNP - A General Monte Carlo Code for Neutron and Photon Transport," Los Alamos Scientific Laboratory Report LA-7396-M, Rev. 2 (September 1986).

4. "CFX 4.1 Flow Solver User Guide," Computational Fluid Dynamics Services, AEA Technology, Harwell Laboratory, Oxfordshire, United Kingdom, October 1995.

5. J.M.McGlaun and S.L.Thompson,"CTH-A Three Dimensional Shock-Wave Physics Code," *Intl. Journal of Impact Engineering*, Vol.10, 251-360, 1990.

6. L. K. Mansur and H. Ullmaier, *Proceedings of the International Workshop on Spallation Materials Technology*, April 23-25, 1996, Oak Ridge, Tennessee, CONF-9604151.